SPALLATION NEUTRON SOURCE PROGRESS, CHALLENGES AND UPGRADE OPTIONS*

Stuart Henderson, Spallation Neutron Source, Oak Ridge National Laboratory, Oak Ridge TN, USA

Abstract

The Spallation Neutron Source accelerator complex consists of a 2.5 MeV H^- front-end injector system, a 186 MeV normal-conducting linear accelerator, a 1 GeV superconducting linear accelerator, an accumulator ring and associated beam transport lines. The design beam power of the SNS is 1.4 MW. Since completion of the construction project in June 2006, attention has focused on increasing the performance of the SNS accelerator complex toward the design parameters. The status of the beam power ramp-up program and present operational limitations will be described. Plans for future upgrades, including a doubling of the design beam power and a second target station, will also be described.

INTRODUCTION

The Spallation Neutron Source (SNS) at Oak Ridge National Laboratory is the world's most powerful short-pulse neutron scattering facility. The SNS construction project was a partnership of six US DOE national laboratories, each of which had responsibility for designing and manufacturing a portion of the facility. At the design beam power of 1.4 MW the SNS will operate at beam powers a factor of 8 beyond that which had been previously achieved [1]. The SNS baseline and present operating parameters are summarized in Table 1.

The SNS accelerator complex consists of a 2.5 MeV H^- injector [2], a 1 GeV linear accelerator [3], an accumulator ring and associated beam transport lines [4]. The injector (also called the Front-End System) consists of an H- volume-production ion-source [5], a Radio-Frequency Quadrupole and a Medium Energy Beam Transport line for chopping and matching the 2.5 MeV beam to the linac. The linear accelerator consists of a Drift Tube Linac (DTL) with 87 MeV output energy, a Coupled-Cavity Linac (CCL) with 186 MeV output energy, and a Superconducting RF Linac (SCL) with 1 GeV output energy [6]. At full design capability the linac will produce a 1 msec long, 38 mA peak, chopped beam pulse at 60 Hz for accumulation in the ring.

The linac beam is transported via the High Energy Beam Transport (HEBT) line to the injection point in the accumulator ring where the 1 msec long pulse is compressed to less than 1 μs by multi-turn charge-exchange injection. According to design, beam is accumulated in the ring over 1060 turns reaching an intensity of 1.5×10^{14} protons per pulse. When accumulation is complete the extraction kicker fires during the 250 nsec gap to remove the accumulated beam in a single turn and direct it into the Ring to Target Beam Transport (RTBT) line, which takes the beam to a liquid-mercury target.

The liquid mercury target system [7] consists of a closed-loop mercury-handling system. The target module is designed for remote-handling maintenance by retraction into a service bay outfitted with remote manipulator systems. Neutrons are moderated in four moderators, one using ambient water, and the other three utilizing supercritical hydrogen at 17-20 K.

The beam commissioning campaign of the SNS accelerator complex was carried out in seven discrete commissioning runs over a four year period. Beam commissioning results are summarized in [8,9].

Formal SNS operations for scheduled neutron scattering experiments began in October 2006. The initial instrument suite was commissioned, and the user program began in 2007. The SNS is now nearly two years into the initial operations phase. It was envisioned to ramp-up the beam power to 1.4 MW, the beam availability to 90%, and the accelerator operating hours to 5000 in the first three years following construction [10].

SNS PERFORMANCE

Table 1 shows a summary of SNS design and operating parameters. The design values refer to the baseline construction project parameters, and the operating values refer to present routine operation.

Table 1: SNS Design and Operating Parameters

	Design	Operating
Beam Power on Target	1.44 MW	0.52
Beam Energy	1.0 GeV	0.88
Linac Beam Macropulse Duty Factor	6.0%	3.0%
Beam Pulse Length	1.0 msec	0.5 msec
Repetition Rate	60 Hz	60 Hz
Peak linac current	38 mA	32 mA
Average Linac H- current	1.6 mA	0.57 mA
Ring accumulation time	1060 turns	530
Ring bunch intensity	1.5×10^{14}	0.5×10^{14}
Ring Space-Charge Tune Spread	0.15	0.05
SRF Cavities	81	75

Figure 1 shows the SNS beam power history. Beam power in routine operation has exceeds 0.5 MW, more than one-third of the design. The beam power has increased by a factor of eight in the last year [10]. Since neutron production in the GeV energy range scales with beam power, the integrated beam power on target is the

*SNS is managed by UT-Battelle, LLC, under contract DE-AC05-00OR22725 for the U.S. Dept. of Energy.

most useful figure of merit for measuring productivity of the accelerator complex. Figure 2 shows the daily integrated beam power, which has climbed to more than 11 MW-hrs delivered per day.

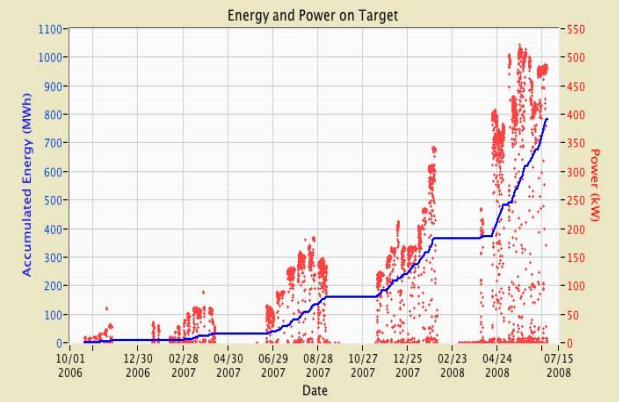

Figure 1: Beam power history of the SNS since the beginning of formal operations in October 2006.

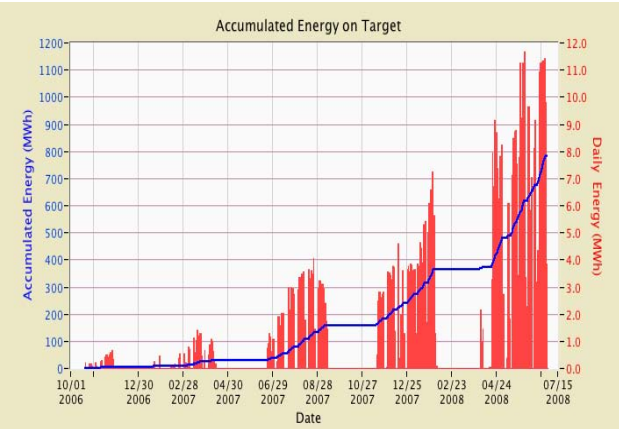

Figure 2: Daily integrated beam power history of the SNS since the beginning of formal operations in October 2006.

OPERATIONAL ISSUES

Front-End Systems

Recent performance of the Front-end and normal-conducting linac are summarized in [11]. The Ion Source routinely delivers peak beam currents in excess of 30 mA. The highest peak current achieved in neutron production is 36 mA, which is near the baseline specification of 38 mA. Antenna lifetime at present 4% duty factor operation exceeds the usual 14-day cycle for scheduled ion source replacement. Nevertheless, an external antenna source has been developed [12] to eliminate the risks associated with operating a water-cooled internal antenna. This source incorporates an elemental Cs system for better control of cesium delivery, as well as a plasma gun.

The Low-energy beam transport (LEBT) system has been responsible for substantial downtime in the past year. The electrostatic design incorporates a segmented four-element lens with the dual function of focusing and chopping. A few-kV pulsed supply is capacitively coupled to each segment of this ~40 kV lens for low-energy chopping. High-voltage arcs of these lens segments direct stored energy toward the chopper driver circuits, leading to failures of driver electronic components. To further protect the driver electronics from such events, an energy-dissipating resistor has been added, which in turn reduces the risetime of the LEBT chopper to ~100 nsec, compared to the specification of 40 nsec. Linac microbunches which arrive during the rise/fall time of the chopper pulse enter the RFQ with large transverse errors that give rise to beamloss downstream.

A new LEBT chopper driver circuit has been built to alleviate these limitations and will be deployed during the next maintenance outage. In the long-term, a magnetic LEBT is being pursued to eliminate the operational issues associated with high-voltage, and chopping at high-voltage [13].

The RFQ RF input distribution system was recently replaced [14]. The previous system utilized eight input couplers to deliver 800 kW peak RF power to the structure. It was difficult to properly balance the drive network so that each input coupler was operating within acceptable average power limits at full duty. This system was replaced with a new one utilizing two high-power couplers, each of which is capable of delivering 400 kW peak power. This system was recently installed, commissioned, and successfully tested at full RF duty cycle, and is now in operation.

The MEBT chopper system was only recently brought on-line for routine operation. The baseline chopper structure, a slow-wave meander-line design, had insufficient capability of handling the small beam power which is deposited on the structure. A straightforward, yet robust, stripline structure was recently installed and is now in routine operation [15]. While the meander line design supported the aggressive ~10 nsec risetime specification for the MEBT chopper system, the stripline structure has about twice the risetime.

The MEBT RF "Rebuncher" system is limited in accelerating gradient, operating about 20% below design in the most critical rebuncher cavity. New MEBT RF amplifiers are being procured.

Linac Systems

The DTL and CCL operate reliably for neutron production. Modifications to improve the resonance-control are underway [16].

The SCL is operating at 0.88 GeV output energy [17]. This is well below the design energy for two reasons. First, six SC cavities are not available for beam acceleration. One cryomodule (containing four cavities) is removed from the tunnel for rework in our SRF maintenance facility. One installed cavity is not operable due to excessive fundamental power transmitted through the HOM coupler [18] and another is not operable due to a faulty field probe signal. Secondly, the average gradient in the high-beta portion of the linac is below the specified

gradient by ~20%. The operating cavity gradients are shown in Figure 3. Cavities in the medium-beta portion of the linac (cryomodules 1-11 in the figure) are operating above the design specification of 10.2 MV/m whereas those in the high-beta portion of the linac (cryomodules 12-23) are operating below the design specification of 15.7 MV/m.

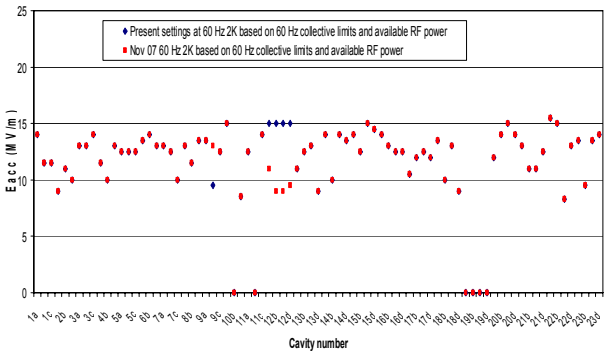

Figure 3: Superconducting cavity operating accelerating gradients. Cryomodule 19 was reworked and installed in slot 12.

Operating gradients are lower than the individual cavity gradient limits [18], due to phenomena denoted "collective effects." With all cavities in one cryomodule powered, we observe field emitted electrons from one cavity transported to adjacent cavities which then deposit energy in poorly cooled regions of the beampipes. The transmission of these field emitted electrons depends on the phases of intervening cavities, therefore the operating gradient for one cavity depends on the surrounding cavities and their phases in a complicated way. For this reason, operating gradients in practice are below those measured for a single cavity.

One cryomodule (CM19) was removed from service last year. This cryomodule had a cavity with excessive fundamental power transmitted through the HOM port, so that it was inoperable above a few MV/m. This cryomodule was repaired by removing and blanking-off the HOM coupler and was subsequently returned to service. All cavities in this cryomodule now operate at 15 MV/m. A second cryomodule was subsequently removed and is undergoing repair in the SRF maintenance facility.

In order to accommodate these absent cavities in the linac lattice, a rapid and powerful method of cavity phase adjustments has been developed [19]. In this method, a model-based algorithm is used to adjust downstream cavity phases in response to a change in upstream cavity setpoints. The method has proven quite useful not only for tuning around missing cavities, but also to make adjustments to cavity gradients for operational reasons.

An effort is underway to develop in-situ surface processing methods (e.g. helium processing) to increase the cavity gradients without full disassembly.

Fourteen modulators [20] utilizing solid-state technology drive 92 klystrons in the linac [21]. These modulators provide 11-MW peak power at 8% duty factor. A number of improvements in the modulator systems are underway to increase their reliability at high duty factor, including a new gate-drive circuit, replacement of transformers and chokes, and utilization of higher power IGBTs.

Linac beamloss and activation

Figure 4 displays the beam loss monitor signals along the linear accelerator during 475 kW operation, overlayed with residual activation measurements. The residual dose rates (mrem/hr) were measured 30 cm from the beamline approximately 24 hours after operating at 475 kW for approximately one week. A number of features are evident. The initial spike in the CCL is from particles outside the DTL acceptance. The steady increase in the latter part of the CCL is a result of the linear optics in which the beam envelopes in the CCL FODO structure are matched to the doublet lattice structure of the SCL. Therefore, the aperture is tightest at this location. Losses and activation near the CCL/SCL transition are evidently due to off-momentum particles outside of the CCL acceptance that are lost at the lattice transition. Efforts are underway to better understand the source of these longitudinal tails. They represent loss rates in the 10^{-5} range, a few times higher than required for 1.4 MW operation.

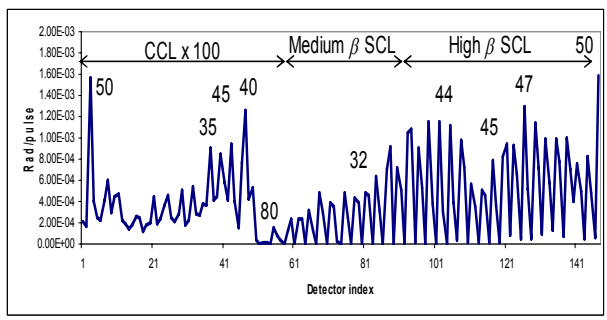

Figure 4: Linac beam loss monitor signals (rads/pulse) recorded during 475 kW operation. Numbers overlayed show residual dose rates (mrem/hr) at 30 cm measured ~24 hours after beam operation.

Accumulator Ring

Present ring performance is summarized in [22]. A number of modifications have been made to the Injection dump line since project completion. A design error was made which had the effect of missteering the beam directed to the Injection Dump when the injection chicane was properly closed for ring injection. A number of improvements have been made to improve transmission to the injection dump; a C-magnet was fabricated and installed to allow independent adjustment of waste beam trajectories; one chicane magnet was moved to place the waste beams in a better field region in the magnet; a larger aperture injection dump septum chamber was installed [23] and the injection septum gap was increased [24]; diagnostics were added to allow measurement of the waste beam trajectories, profiles and beam current. As a result of these modifications, the losses are improved

substantially (see below). Further improvements forthcoming in the injection region include a thinner secondary stripping foil and modified primary foil handling mechanism for ease of active handling.

The extraction septum magnet has been identified as the source of coupling responsible for a small tilt of the beam profile in the RTBT [24, 25].

HEBT/Ring/RTBT Beamloss

The beamloss monitor signals and measured residual activation in the HEBT, Ring and RTBT are shown in Figure 5. Several features are evident. First, the highest residual activation is located near the primary stripping foil, as is expected. The injection dump line levels are elevated due to a thick secondary foil. Losses in the extraction region (joining Ring and RTBT) are higher than normal during this running period due to an improperly functioning LEBT chopper system. Extraction losses can be reduced through use of Ring RF adjustments [26]. The highest residual activation in the HEBT is near the first dipole magnet, suggesting that off-momentum particles are swept-out at this location.

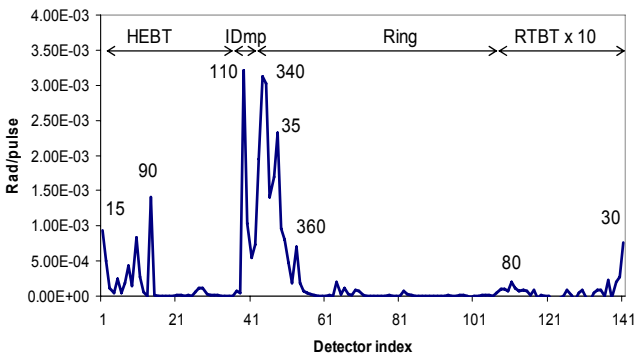

Figure 5: HEBT/Ring/RTBT beam loss monitor signals (rads/pulse) recorded during 475 kW operation. Numbers overlaid show residual dose rates (mrem/hr) at 30 cm measured ~24 hours after beam operation.

AVAILABILITY

Neutron production beam availability since the initiation of formal operations is shown in Figure 6. Each bar shows the availability (delivered hours/scheduled hours) during each neutron production running period. The initial running in 2006 was comprised of three-day neutron production periods, whereas from early 2007 onward neutron production run lengths are 9 to 11 days in duration. The initial availability, at low duty factor and beam power was in excess of 75%. In winter 2007 availability suffered as a result of electrostatic LEBT high-voltage arcs and subsequent chopper damage. Once mitigated the availability increased to an average level of ~85%. Some failures with lengthy mean-time-to-repair led to reduced availability in spring 2008. Subsequently the availability has recovered to ~80%, running at ~0.5 MW beam power. Downtime in the last year has been dominated by linac modulator systems.

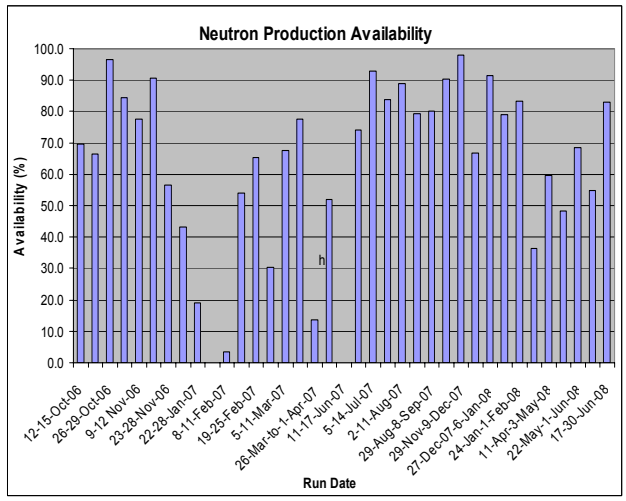

Figure 6: Neutron production availability (%) for each run period since the beginning of formal SNS operations. Run lengths vary from 3 days in 2006 to 11 days at present.

SNS POWER UPGRADE PROJECT

The Power Upgrade Project plan calls for a doubling of the beam power capability of the accelerator, increasing the proton beam power to at least 2 MW with a design goal of 3 MW. The Power Upgrade will enable operation of a second, long- wavelength target station (LWTS), thereby doubling the scientific capability of the facility. Table 2 compares parameters for the initial baseline SNS accelerator complex (1.44 MW) with the Beam Power Upgrade (3 MW). The Power Upgrade Project is described in more detail in [27]. The Project is seeking CD-1 approval, and anticipates construction beginning in 2011 with completion in 2016.

A straightforward increase in SNS beam power to 3 MW can be realized by i) increasing the linac beam energy from 1.0 to 1.3 GeV by installing nine additional high-beta superconducting cryomodules, and ii) increasing the H^- ion source pulsed current (measured at RFQ output) from 38 mA to 59 mA. We have chosen to maintain the present 6% linac beam duty factor. With only a few exceptions, the ring and transport line hardware have been designed and built for 2 MW of beam power at 1.0 GeV, and with the capability of 1.3 GeV operation. Therefore, the 3MW SNS upgrade, while certainly containing challenging aspects, can nevertheless be considered an extension of the present SNS design.

It is important to recognize that from the standpoint of space-charge effects, the upgrade parameters are no more challenging than those of the baseline. Due to the strong dependence on particle velocity, the space-charge tune-shift at 1.3 GeV for 3MW parameters is identical to that at 1 GeV for 1.4 MW parameters.

Table 2: SNS Baseline and Power Upgrade Parameters

	Baseline	Upgrade
Kinetic energy [MeV]	1000	1300
Beam power [MW]	1.4	3.0
Chopper beam-on duty factor [%]	68	70
Linac beam macro pulse duty factor [%]	6.0	6.0
Average macropulse H- current [mA]	26	42
Peak macropulse H- current [mA]	38	59
Linac average beam current [mA]	1.6	2.5
SRF cryo-module number (med-beta)	11	11
SRF cryo-module number (high-beta)	12	21
SRF cavity number	33+48	33+84
Peak surface gradient (β=0.81 cavity) [MV/m]	35 (+2.5/-7.5)	31
Ring injection time [ms] / turns	1.0/1060	1.0/1100
Ring rf frequency [MHz]	1.058	1.098
Ring bunch intensity [10^{14}]	1.6	2.5
Ring space-charge tune spread, ΔQ_{SC}	0.15	0.15
Pulse length on target [ns]	695	691

SECOND TARGET STATION

With a doubling in the SNS beam power enabled by the Power Upgrade Project, operation of a second target station will be enabled. In the reference concept [28], the accelerator will deliver 20 long-pulses per second to the second target station and 40 short pulses per second to the first target station. In this mode, 1 MW beam power is delivered to the second target station and 2 MW to the first.

An additional transfer line, not included in the Power Upgrade Project, will be required to transport beam to the second target station.

CONCLUSION

The SNS construction project was completed in June 2006. The SNS began formal operations in October 2006, which also marks the beginning of an anticipated three-year ramp-up toward the full design performance. The SNS is making rapid progress, having achieved 0.52 MW delivered to the neutron production target. This power level keeps the SNS on-track with ramp-up goals, and makes the SNS the world's most powerful pulsed spallation neutron source. Plans are underway for increasing the beam power beyond the design specification to 3 MW through the SNS Beam Power Upgrade Project, which is presently seeking DOE CD-1 approval.

ACKNOWLEDGEMENTS

The author gratefully acknowledges the hard work and dedication of the entire SNS staff which made possible the results presented herein.

REFERENCES

[1] D. Findlay, Proc. PAC 2007, p. 695.
[2] A. Aleksandrov, Proc. PAC 2003, p. 65
[3] D. Jeon, Proc. PAC 2003, p. 107
[4] J. Wei, Proc. PAC 2003, p.571
[5] R.F. Welton, et al., Proc. PAC 2005, p. 472; M. Stockli, Proc. LINAC06, p. 213
[6] I.E. Campisi, Proc. PAC 2005, p. 34
[7] T. Gabriel, et al., Proc. PAC 2001, p. 737.
[8] S. Henderson, Proc. ICFA HB2006, p. 6
[9] S. Henderson, Proc. LINAC 2006, p. 1
[10] S. Henderson, Proc. PAC 2007, p. 7.
[11] A. Aleksandrov, et al., these proceedings, THPP073.
[12] R. Welton, et al., Proc. PAC 2007, p. 3774.
[13] B.X. Han and M. Stockli, Proc. PAC 2007, p. 1823.
[14] Y. Kang, et al., these proceedings, MOPP091.
[15] A. Aleksandrov, et al., Proc. PAC 2007, p. 1817.
[16] D. Williams, et al., these proceedings, MOPP110.
[17] Y. Zhang, et al., these proceedings, THPP044.
[18] I. Campisi, et al., Proc. PAC 2007, p. 2502.
[19] J. Galambos, et al., Proc. PAC 2007, p. 885.
[20] D. Anderson, Proc. LINAC 2006, p. 541.
[21] M. Champion, Proc. PAC 2007, p. 3792.
[22] M. Plum, et al., these proceedings, THPP085.
[23] G. Murdoch, these proceedings, TUPD034.
[24] J.G. Wang, these proceedings, WEPC163.
[25] S. Cousineau, et al., these proceedings, THPC006; J. Holmes, et al., these proceedings, THPC015.
[26] Y. Zhang and J. Galambos, these proceedings, MOPC136.
[27] S. Henderson, et al., Proc. EPAC 2006, p. 345.
[28] K. Crawford (ed.), « A Second Target Station for the SNS », ORNL Internal Note